Traveling Wave Locomotion of Snake Robot along Symmetrical and Unsymmetrical body shapes

Hadi kalani[1], Alireza Akbarzadeh[2], Javad Safehian[3]
1 Ferdowsi University of Mashhad, Mashhad, Iran. Hadi.kalani@yahoo.com
2 Ferdowsi University of Mashhad, Mashhad, Iran. Ali_akbarzadeh_t@yahoo.com
3 Ferdowsi University of Mashhad, Mashhad, Iran. Safehian_javad@yahoo.com

Abstract

In this paper, kinematics and dynamics of traveling wave locomotion of a snake robot with two types of body shapes are developed. The body shape, also called body curve, is the actual geometrical shape in the plane in which the robot can assume during its progression. The snake can then travel along this curve. Two types of body curves, symmetrical and unsymmetrical, have been introduced for creeping locomotion, in horizontal plane [4]. Kinematics and dynamic of traveling wave with symmetrical body curve has also been developed [2]. These concepts are applied and kinematics and dynamics for traveling wave in vertical plane with unsymmetrical body shapes are obtained.

In kinematics section, we first determine the joint relative angles using the body shape and curvature function [1]. Next, position, velocity and acceleration of each link as well as center of gravity of the snake body are calculated. In Dynamic's section, force diagram of the i^{th} link is shown. Using Newton principle, relative motion of the i^{th} link with respect to the $(i+1)^{th}$ link is determined. Next, effects of friction coefficient, initial winding angle and the unsymmetrical factor on the joint torques are investigated. Results indicate that as the winding angle increases, joint torques decreases. Additionally, it is shown that the unsymmetrical factor, k, does not significantly affect torques. Finally, to validate our analysis, traveling wave locomotion is simulated in both Webots as well as MATLAB. It is shown that the traveling wave locomotion for both symmetrical and unsymmetrical body shapes is realized.

Key words: Snake Robot, Traveling wave, Symmetrical and Unsymmetrical serpenoid curve, winding angle.

1 Introduction

The sizable elongation of their body and the particular mode of locomotion have allowed snakes to expand into various environments. This makes snakes adaptable to a given environment and be able to perform many kinds of movements. Snake robot gaits, a type of locomotion, can be subdivided into two main classes: Snake-like and non-snake-like gaits. Serpentine, concertina and sidewinding are three most common snake-like gaits which are inspired from real snakes. Non-snake-like gaits do not exist in nature but are applicable in snake robot locomotion. However, these gaits are less addressed in literatures. Spinning gait, flapping gait and traveling wave gait are some examples of such gaits. Travelling wave locomotion occurs in vertical plane orthogonal to the supporting plane. Thus, in vertical locomotion, its motion width is approximately equal to its body section.

One of the original studies of snake-like robots was conducted by Hirose [1]. He approached the problem from a biologically inspired aspect and formulated serpenoid curve. He also proved that a snake-like mechanism is able to generate a net forward thrust by applying the appropriate torque along the length of its body. Hirose also built a wheel-based, snake-like robot successfully using these results. Chen et al. [2] presented a model for traveling wave locomotion and considered its kinematics and dynamics. They considered the joint torques during traveling wave locomotion and the effects of the initial winding angle and friction coefficient on the joint torques. Chen et al. [3] also analyzed the mechanism of traveling wave locomotion of a snake robot and showed that one period of this locomotion can be divided in four phases. They showed that these phases are based on the number of joints contacting the supporting surface and the resultant of the friction forces on contacting joints. During movement, values of friction forces of the two contacting points are different. The difference between friction forces, resultant force, is the force that generates locomotion. Ma et al. [4] studied influence of different slopes on creeping locomotion along symmetrical and unsymmetrical body shapes. By comparing results of the symmetrical body curve and that of the unsymmetrical body curve, they demonstrated that the unsymmetrical body curve increases robot's performance while the required joint torques remain mostly unchanged. Date et al. [5] discussed dynamic manipulability for a snake-like articulated robot. They suggested a simple controller for an autonomous locomotion which is capable of tracking a desired trajectory using their proposed manipulability. Ma et al. [6] formulated the kinematics and the dynamics of three dimensional snake robot and analyzed creeping locomotion. Consequently they showed that the robot moves at higher speed in the sinus-lifting creeping motion mode with curvature-weighted normal reaction forces than with

uniform normal reaction forces. Ma et al.[7] investigated the creeping propulsion, in lateral locomotion, which is the most frequently used type of snakes motion.
Paap et al. [8] described their robot and focused on a method for motion control that allows a flexible and robust method of path planning. Their method applies not only to snake-like movement but also to any wheeled robot which is able to control the curvature of its path. Ostrowski and Burdick [9] analyzed a model, based on Hirose's Active Cord Mechanism (ACM). Using kinematics constraints, they developed a connection that describes the net motion of the machine as a function of variations in the mechanism shape variables. They also discussed how these algorithms can be used to optimize certain inputs given the particular choice of physical parameters for a snake robot.

In this paper, first we define symmetrical and unsymmetrical serpenoid curves. Next, we consider kinematics and the dynamics of traveling wave locomotion in vertical plane of snake robot along both body curves.

2 Analysis of snake-like locomotion

Body shape of snake is described by a series of S-shaped, sinusoidal-like curves that the body forms while in execution. In most robots, this motion is usually mimicked by the utilization of serpenoid curve, introduced by Hirose, and using passive wheels to resist lateral movement of the robot's segments [1].Serpenoid curve is shown in Figure 1.

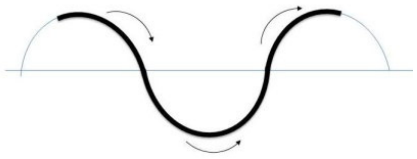

Figure 1 serpenoid curve

2.1 Symmetrical Body Shape

For convenience, we use the serpenoid curve [2, 3, and 4] that is a symmetrical curve, as the basic body shape of the snake robot. The Serpenoid curve is given by the curvature function:

$$\rho(s) = \frac{-2K_n\pi\alpha}{L}\sin\left(\frac{2K_n\pi s}{L}\right) \tag{1}$$

Where L is the whole length of snake body, K_n is the number of the wave shapes, α is the initial winding angle of the curve and s is the body length along the body curve, as shown in Figure 2. The snake robot consists of n links with element of unit length l that is connected through n-1 joints. While snake moves in a plane, we assume that any change to the serpenoid curve is followed by a corresponding change in snake robot body shape. In other words, the snake keeps its shape on the serpenoid curve.

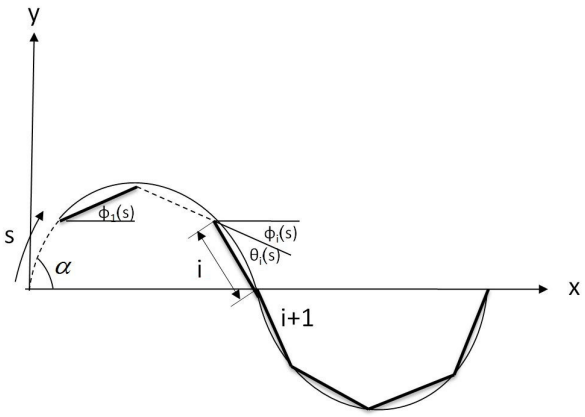

Figure 2 Scheme for fitting the serpenoid curve

Consider Figure 2. The joint variables, specifically relative angles $\theta_i(s)$, may be regarded as the shape control variables. The joint variables can be derived from the integration of the curvature formula as,

$$\theta_i(s) = -2\alpha\ \sin\left(\frac{K_n\pi}{L}\right)\times\sin\left(\frac{2K_n\pi s}{L}+\frac{2K_n\pi i}{l}-\frac{K_n\pi}{n}\right) \tag{2}$$

Where l is the unit length of link, n is the number of links and s is the virtual displacement of the tail along the serpenoid curve path. The virtual displacement, s, decides the changing frequency of the body curve. The relative angle velocities and accelerations can be derived by differentiating Equation 2 with respect to time. Using the relation between values of absolute and relative joint angles, we obtain:

$$\phi_i = \phi_1 + \sum_{k=1}^{i-1}\theta_k, i = 1,2,..., n \tag{3}$$

Where ϕ_1 is absolute angle for the 1st link and ϕ_i are absolute angles of subsequent links. The absolute velocities and accelerations can be derived by differentiating Equation 4 with respect to time. It should be noted that, during locomotion, when s is given, ϕ_1 can be calculated [1] as follows,

$$\phi_1 = \alpha\cos\left(\frac{2\pi\ \mathrm{K_n\ s}}{\mathrm{L}}\right) \tag{4}$$

2.2 Unsymmetrical Body Shape

Unsymmetrical body shape may be realized by changing the initial winding angle relative to each joint. Doing this will result in a modified serpenoid curve, also called unsymmetrical body shape. The initial winding angle is defined as,

$$\alpha(i) = \frac{\pi}{180}ki + \alpha \tag{5}$$

Where i represents the number of links and k is unsymmetrical factor. By rewriting Equation 2, we will have

$$\rho(s) = \frac{-2K_n \pi\alpha(i)}{L} \sin(\frac{2K_n \pi s}{L}), i = 1,2,..., n \quad (6)$$

By changing k and the initial value of the winding angle, α, an unsymmetrical curve can be generated [4]. Figure 3 shows examples of the unsymmetrical curves using different value of the unsymmetrical factor k when α is $\pi/6$.

3 Kinematics of snake robot

To define a kinematics model for the robot, we attach a coordinate system to each link of the robot. See Figure 4. The displacements of the joints and the displacements of the gravity centres of links can then be given by,

$$^{i+1}r = {}^0r + \sum_{j=0}^{i} l_j \begin{bmatrix} c_j \\ s_j \end{bmatrix}, \; ^i r_G = {}^i r + l_{Gi} \begin{bmatrix} c_j \\ s_j \end{bmatrix} \quad (7)$$

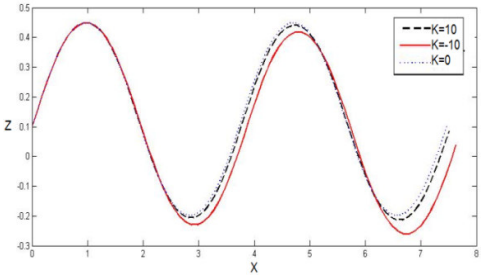

Figure 3 Effect of unsymmetrical factor k on body curves when α is $\pi/6$

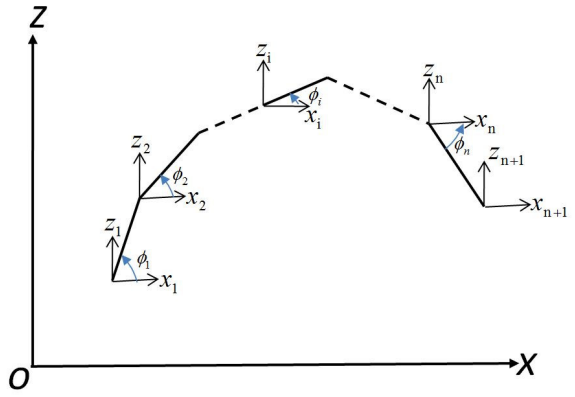

Figure 4 Coordinates located on the snake-like robot

Where l_i is the length of link i, l_{Gi} is the distance to gravity center of link i, and $i = 1, 2, 3,...,$ n and n represents the total number of links. Velocity and acceleration of the center of gravity for each link can be derived by time-differentiation of Equation 6. For simplicity of formulations, we set $s_k = \sin(\phi_k)$ and $c_k = \cos(\phi_k)$.

4 Dynamics of snake robot

The dynamics of the snake robot can be viewed as a combination of mechanism dynamics and environment constraints. The objective of mechanism dynamics is to model the functional relationship between the joint torques and the robot locomotion. The interaction forces between the body and the environment can be determined by environment constraints. The dynamics of the snake robot presented in this paper has been derived using Newton-Euler formulation. Consider the planar snake robot depicted in Figure 4, which consists of n links connected through n-1 joints. Each link is rigid with uniformly distributed mass and is equipped with a torque actuator (motor), mass m_i, length l_i, and moment of inertia $I_i = m_i l_i^2/3$. Let (x_i, z_i) and ϕ_i define the center of gravity and the angle between the link and the x-axis, respectively. Free-body diagram for the i^{th} link is shown in Figure 5.

Where $N_{i,i+1}$, $F_{i,i+1}$, are the supporting force and friction force of the i^{th} link on the $(i + 1)^{th}$ joint, respectively. Also T_i, f_i, m_i and I_i represent torque, internal force, mass and moment of inertia of the i^{th} link, respectively. Finally, F_{ii} is the friction force of the i^{th} link on the i^{th} joint.

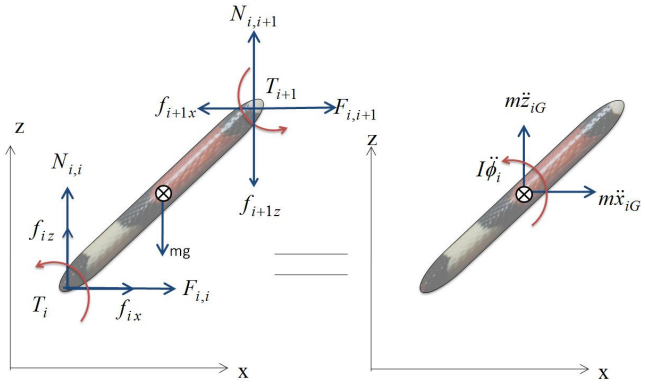

Figure 5 Free body diagram of i^{th} link

Applying the Newton's second principle to the free-body diagram of the i^{th} link in Figure 5 and expanding it to n number of links, we can obtain translational and rotational equations of motion [2].

$\sum F_x = m\ddot{X}_G \rightarrow f_{ix} - f_{i+1x} + F_{i,i} + F_{i,i+1} = m\ddot{x}_{iG}$	(8)
$\sum F_z = m\ddot{Z}_G \rightarrow f_{iz} - f_{i+1z} + N_{i,i} + N_{i,i+1} - mg = m\ddot{z}_{iG}$	(9)
$\sum M = I\ddot{\phi} \rightarrow \tau_i - \tau_{i+1} + (f_{ix} + f_{i+1x} + F_{i,i} - F_{i,i+1}) l \sin\phi_i / 2$ $- (f_{iz} + f_{i+1z} + N_{i,i} - N_{i,i+1}) l \cos\phi_i / 2 = I_i \ddot{\phi}_i$	(10)

Because both the head and the tail links of the snake robot are free, we can infer the followings

$$f_{1x} = f_{1z} = f_{n+1x} = f_{n+1z} = 0 \quad (11)$$

$$\tau_1 = \tau_{n+1} = 0 \quad (12)$$

Note that the trace of all links are along the serpenoid curve however, the displacement of the whole body is a

straight line along the X-axis. By taking second derivative of Equation 7, placing Equations 11 through 12 into Equations 8 through 10 and simplifying we can obtain

$$mn\ddot{x}_1 - m\sum_{i=1}^{n}\left\{\sum_{k=1}^{i-1}(l\cos(\phi_k)\dot{\phi}^2{}_k + l\sin(\phi_k)\ddot{\phi}_k) + \frac{l}{2}\cos(\phi_i)\dot{\phi}^2{}_i + \frac{l}{2}\sin(\phi_i)\ddot{\phi}_i\right\} = \sum_{i=1}^{n}F_i \quad (13)$$

$$n\ddot{z}_1 - \sum_{i=1}^{n}\left\{\sum_{k=1}^{i-1}(l\sin(\phi_k)\dot{\phi}^2{}_k - l\cos(\phi_k)\ddot{\phi}_k) + \frac{l}{2}\sin(\phi_i)\dot{\phi}^2 - \frac{l}{2}\cos(\phi_i)\ddot{\phi}_i\right\} = 0 \quad (14)$$

$$\sum_{i=1}^{n}\left\{(2\sum_{j=i}^{n}m\ddot{x}_j - m\ddot{x}_i - 2\sum_{j=i+1}^{n+1}F_j)l\sin\phi_i/2 - (2\sum_{j=i}^{n}m\ddot{z}_j - m\ddot{z}_i - 2\sum_{j=i+1}^{n+1}N_j + (2n+1-2i)mg))l\cos\phi_i/2\right\} = \sum_{i=1}^{n}I_i\ddot{\phi}_i \quad (15)$$

Where $F_j = F_{j-1,j} + F_{j,j}$ and $N_j = N_{j-1,j} + N_{j,j}$ represent the friction force and the supporting force of the j^{th} joint. Equations 13 and 14 represent the relation between the linear $\ddot{z}_1, \ddot{x}_1$, and angular acceleration, $\ddot{\phi}_1$, of head of robot or the 1st link. Equations 13 through 15 represent three equations and three unknowns. By simultaneously solving these equations we can obtain $\ddot{x}_1, \ddot{z}_1$ and $\ddot{\phi}_1$. Next the head link joint angle, ϕ_1, and its angular velocity, $\dot{\phi}_1$, as well as velocity of the head , $\dot{x}_1$ and $\dot{z}_1$, and its moving distance, x_1 and z_1, are all obtained through integration. Once these variables are calculated, the kinematics of the remaining snake robot links may be obtained. Therefore, if parameters that define body curve, such as α , s, K_n, l are defined, then parameters that define robot motion can be obtained.

Next, we need to obtain the necessary motor torques to result in the desired motion. To do this, we can place Equations 8 and 9 into 10 and upon simplifying we can obtain,

$$\tau_i - \tau_{i+1} + (2\sum_{j=i}^{n}m\ddot{x}_j - m\ddot{x}_i - 2\sum_{j=i+1}^{n+1}F_j)l\sin\phi_i/2 - (2\sum_{j=i}^{n}m\ddot{z}_j - m\ddot{z}_i - 2\sum_{j=i+1}^{n+1}N_j + (2n+1-2i)mg))l\cos\phi_i/2 = I_i\ddot{\phi}_i \quad (16)$$

4.1 Interaction of robot with environment

A snapshot of a snake robot traveling in a wave locomotion mode is shown in Figure 6. During traveling wave locomotion, as links travel through the body curve, there are instances when full length of each link becomes in contact with ground. This time is assumed to be significantly low and thus negligible. Further, in this paper, we assume that there are two contact points with ground and subsequently two friction forces. To generate locomotion, the resultant of these two friction forces should be high enough to transmit traveling wave. The velocity of this locomotion is dependent on the transmitting velocity of the wave along the body. The values of friction forces are dependent on the body shape that decides the amount of pressure on the supporting plane. To model the friction forces, we consider a simple coulomb friction as

$$F_i = -\mu.sign(v).N_i \quad (17)$$

Where μ is the friction coefficient between the contacting joint and the supporting plane. The function is denoted by sign(x); i.e. 1 if x>0, 0 if x=0 and -1 if x<0.

Consider Figure 6, Newton second principle is applied to the free-body diagram of snake robot. Therefore,

$$N_u = \frac{1}{d}\left[(G + M\ddot{Z}_G)(x_G - x_{u'}) - M\ddot{X}_G z_G\right] \quad (18)$$

$$N_u = G - N_{u'} \quad (19)$$

Where d is the distance between the two supporting points, $M\ddot{X}_G$ and $M\ddot{Z}_G$ are the inertial forces of the body along the X-axis and Z-axis, respectively. The gravity center of the snake robot should be between the two contact points, in order to stay balanced.

5 Computer Simulation

In this section, the traveling wave locomotion along a symmetrical and unsymmetrical body shape is simulated. The variations of the joint torques with time are depicted, and the effects of friction coefficient, initial winding angle and unsymmetrical factor of the body shapes on the joint torques are discussed.

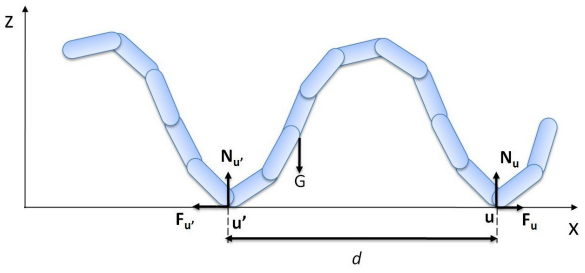

Figure 6 External forces on the snake body

5.1 Simulation conditions

The robot model used in simulation is assumed to have 16 links and 15 joints. Each joint has one rotational degree of freedom around axis $\hat{e}_{yi}$ with angle ϕ_{yi} . Each link is considered to be a solid rectangular beam. Table 1 shows the parameters used in the simulation. To define a body shape, the serpenoid curve parameters shown in table 2 are used.

Table1 Simulation parameters

Link length, l [m]	0.1
Number of links, n	16
Mass of a each link, m[kg]	0.1
Coef. of dynamic friction,μ	0.3

Table2 Serpenoid Curve Parameters

Initial winding angle	$\pi/6$
Total Length of snake	1.6
Number of S-shape k_n	2.0

The body curve is changed with regards to s, $\dot{s}$ and $\ddot{s}$. The acceleration, $\ddot{s}$, is given by

$$\ddot{s} = \begin{cases} a & 0 \le t < T/10 \\ 0 & T/10 \le t < 9T/10 \\ -a & 9T/10 \le t < T \end{cases} \quad (20)$$

Where T is the simulation time and a is the desired acceleration. These values are assumed to be 20 seconds and 0.0625 m/s^2, respectively.

Further, the initial winding angle is assumed to be $\phi_1 = \alpha$. The initial position and initial velocities are selected as $x_1 = z_1 = 0$ and $\dot{x}_1 = \dot{z}_1 = 0, \dot{\phi}_1 = 0$, respectively.

5.2 Results

MATLAB software is used for simulation. Dynamic Equations 13 to15 are used and outputs such as joint angles, joint torques and trace of snake robot with respect to time is determine.

5.2.1 Joint angle

The absolute angle of each joint during simulation is shown in Figure 7. Each color represents a single joint. The head link of the snake is shown with the dark blue color. Also, the figure reveals the sinusoidal nature of the changes in joint angles as well as the constant phase difference between joints.

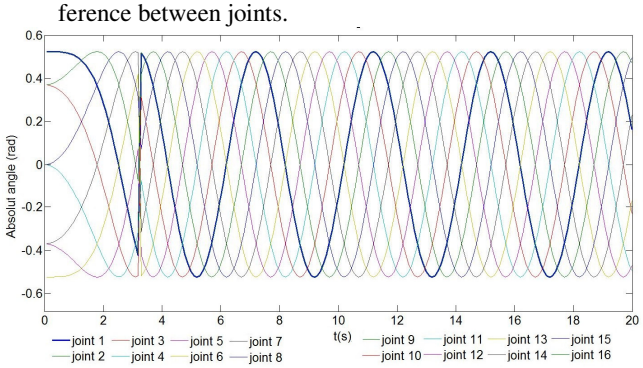

Figure 7 Changes in joint angles for 16 joints with respect to time

5.2.2 Trace of snake robot

The trace of snake robot in traveling wave locomotion is shown in Figure 8. It can be seen that the trace of every link is along the serpenoid curve, while the displacement of the whole body is a straight line along the X-axis.

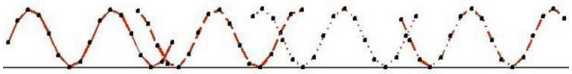

Figure 8 The trace of snake robot in traveling wave locomotion

5.2.3 Joint torques for symmetrical and unsymmetrical body shapes

The changes in joint torques for joints 3, 7, 9, 13 and symmetrical body shapes are shown in Figure 9. As can be seen, joint torques are periodic and amount of maximum joint toques for joints 3, 7 and 9 are in increasing order while joint 13 is lower. This is because joint 9 is the nearest joint to the gravity center of the snake robot. In other words, as joints get closer to the center of gravity, the required maximum torque increases. This finding is similar to what is reported in the earlier literature [2].

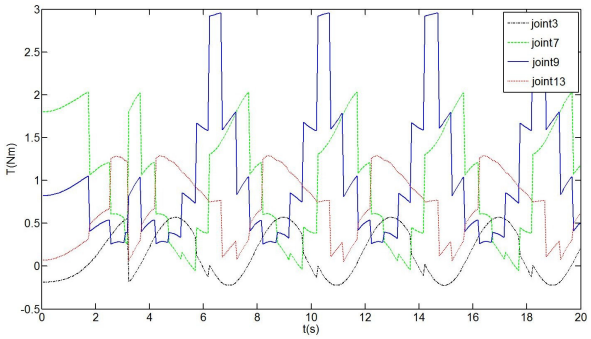

Figure 9 Joint torques when $\alpha = \pi/3, \mu = 0.3$

The same comparison is made for the case of unsymmetrical body shape. Results, as shown in Figure 10, are similar to the case of symmetrical body shape.

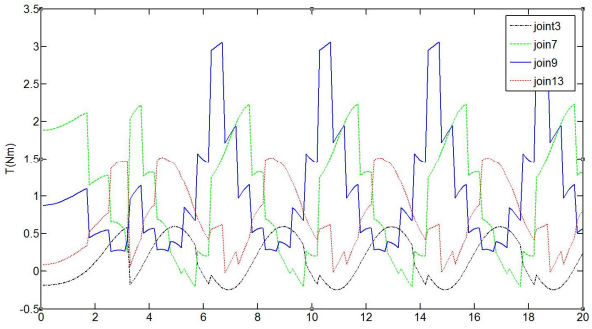

Figure 10 Joint torques when $\alpha = \pi/3, \mu = 0.3$ and $k = 10$

5.2.4 Effect of environment on the joint torques

To study the effect of changing environment, changes in friction coefficient, on the joint torques, we will select joint number 9. This joint was selected because it exhibited the most amount of required torque. To demonstrate the effect, winding angle is assumed to be fixed, $\alpha = \pi/6$ and μ is varied from 0.1, 0.3, and 0.5 to 0.7. Joint torque for two cases, symmetrical and unsymmetrical body shapes are considered. As expected and shown in Figures 11 and 12 keeping the initial winding angle fixed, the required joint torques are increased with the increasing of friction coefficient.

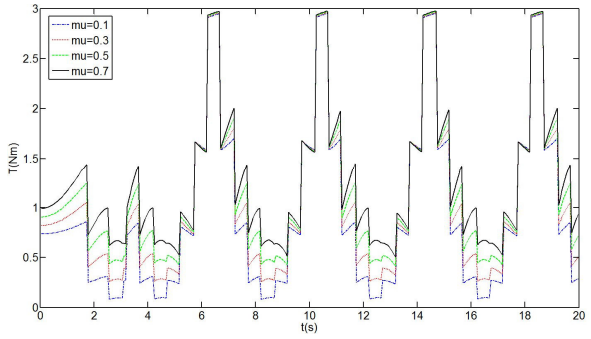

Figure 11 Effect of environment on torque of joint #9

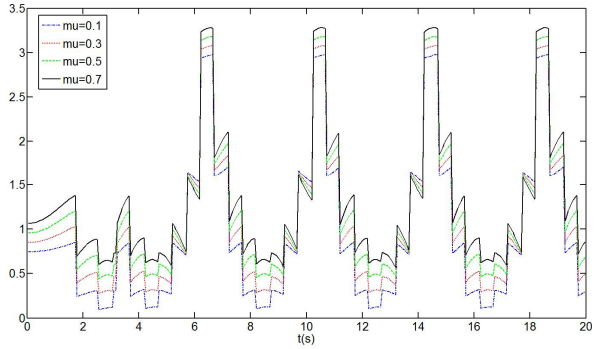

Figure 12 Effect of environment on torque of joint #9, when k=3

5.2.5 Effect of the initial winding angle on the joint torques

As can be seen in Figures 13 and 14 when $\mu = 0.3$ and α is chosen as $\pi/12, \pi/6, \pi/4$ and $\pi/3$, keeping the coefficient of friction fixed, the required joint torques are decreased with increasing of the initial winding angle. This is because increasing the initial winding angle increases the distance between supporting forces. This in turn results in a lower required joint torques. Therefore, if a snake robot is in an environment where friction coefficient is larger, then one control strategy for locomotion may be to increase the winding angle to reduce the required joint torques. As before, joint torque for two cases, symmetrical and unsymmetrical body shapes are considered.

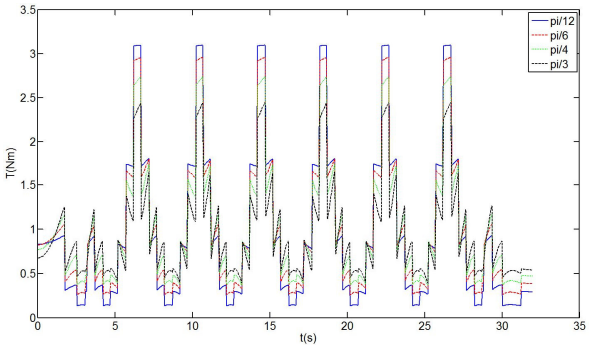

Figure 13 Effect of initial winding on torque of joint #9 when k=0

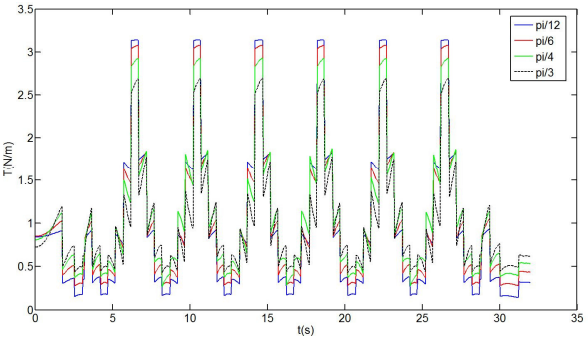

Figure 14 Effect of initial winding angle on torque of joint #9 when k=3

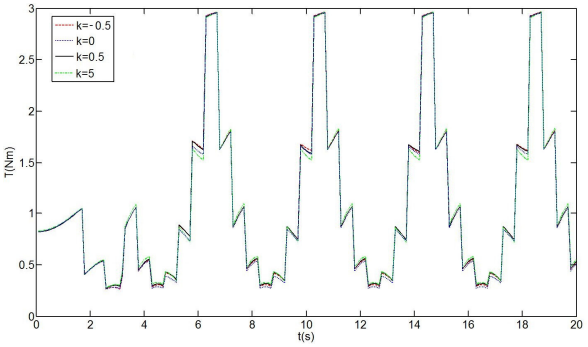

Figure 15 Effect of unsymmetrical factor on torque of joint #9

Also, as it is shown in Figure 15, unsymmetrical factor, *k*, does not significantly affect torques.

5.2.6 Simulation of snake robot in Webots

For simulation both, symmetrical and unsymmetrical body shapes are considered. Webots™ software is used for simulation. Webots™ is a popular commercial software used for mobile robotics simulation and provides a rapid prototyping environment for modeling, programming and simulation. A snap shot of our 16 link snake robot moving in traveling wave locomotion is shown in Figure 16.

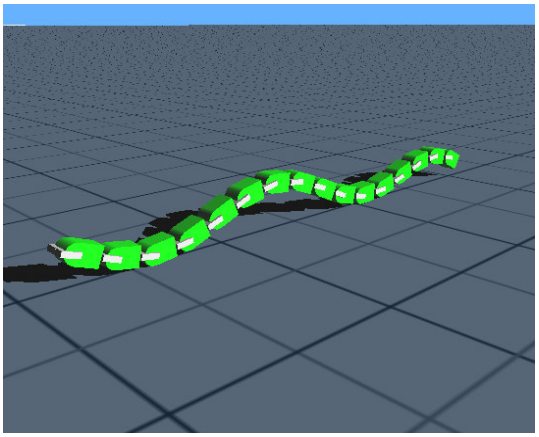

Figure 16 Simulation of snake robot in Webots

Two different cases are studied; symmetrical and unsymmetrical body shapes for travelling wave locomotion. All variables such as friction, winding angle, snake parameters such as length, width, and mass, as well as the virtual displacement and its derivatives are assumed fixed during the 20 seconds simulation time. The displacement of the mass center of the robot is recorded for the two cases. For unsymmetrical case mass center progresses 0.81m while for the symmetrical case it progresses 0.57m. This represents a significant increase in snake robot speed when unsymmetrical body shape is considered. Figures 17 and 18 show the snake-robot in traveling wave locomotion with symmetrical and unsymmetrical body shapes, respectively.

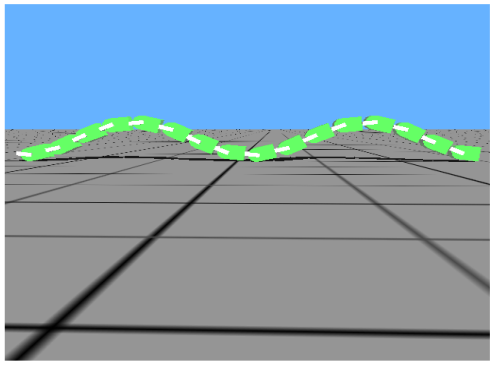

Figure 17 Snake robot along symmetrical curve

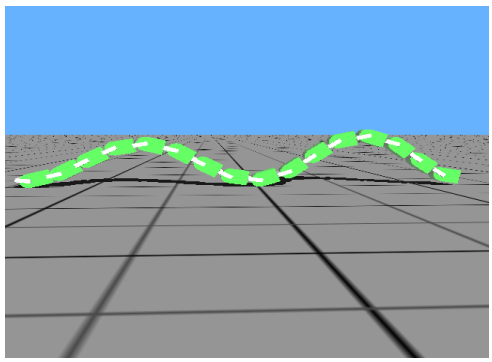

Figure 18 Snake robot along Unsymmetrical curve

6 Conclusion

In this paper, kinematics and dynamics of traveling wave locomotion of a snake robot with two types of body shape are studied. We first introduced a novel locomotion, namely unsymmetrical body shape in traveling wave locomotion. To do this, we combined unsymmetrical body shape used for serpentine locomotion and kinematics modeling of traveling wave. Next, dynamic model of snake robot in a unsymmetrical traveling wave locomotion was developed and formulated in MATLAB software. Using the dynamic equations, effect of changes in winding angle, coefficient friction and unsymmetrical factor on joint torques were investigated. Results indicates increase of winding angle, decreases the required joint torque while increase in friction increase the required joint torques. We also showed that both unsymmetrical and symmetrical body shapes consume about equal amount of torques. Last, a model of the snake robot was developed in Webots software. Through simulation, we showed that, for the same input torque, the slightly unsymmetrical body curve progresses significantly more, 42%, than the symmetrical body shape.

7 Literature

[1] S. Hirose, *Biologically Inspired Robots (Snake-like Locomotor and Manipulator)*, Oxford University Press, 1993.

[2] Li Chen, Shugen Ma, Yuechao Wang, Bin Li, *Design and modeling of a snake robot in traveling wave locomotion*, Mechanism and Machine Theory 42 (2007) 1632–1642.

[3] Li. Chen, Yuechao. Wang, Shugen. Ma, Bin. Li, *Analysis of Travelling Wave Locomotion of Snake Robot*, Proc. International Conference on Robotics Intelligent Systems and Signal Processing, Changsha, China - October 2003.

[4] Shugen Ma, Naoki Tadokoro, Kousuke Inoue, Bin Liz, *Influence of Inclining Angle of a Slope to Optimal Locomotion Curves of a Snake-like Robot*, Proceedings of the 2003 IEEE Changsha, China - October 2003 International Conference on Robotics, intelligent Systems and Signal Processing.

[5] H.Date, Y.Hoshi, and M.Sampei, *Locomotion Control of a Snake-Like Robot based on Dynamic Manipulability*, Proceedings of the 2000 IEEE/RSJ International Conference on Intelligent Robots and Systems.

[6] Shugen. Ma,Yoshihiro. Ohmameuda, Kousuke, Inoue, *Dynamic Analysis of 3-dimensional Snake Robots*, Proceedings of 2004 IEE /RSJ International Conference on Intelligent Robots and Systems, September 28 -October 2,2004, Sendai, Japan.

[7] S. Ma, H. Araya, L. Li, *Development of a creeping locomotion of snake-like robot*, Int. J. Robotics Autom. 17 (4) (2002) 146–153.

[8] K.L. Paap, M. Dehlwisch, B. Klaassen, *GMD-Snake, A Semi-Autonomous Snake-like Robot*, Distributed Autonomous Robotic Systems, 2, Springer-Verlag, Tokyo, 1996.

[9] Jim. Ostrowski, Joel. Burdick, *Gait Kinematics for a Serpentine Robot*, Proceedings of the1996 IEEE International Conference on Robotics and Automation, Minneapolis, Minnesota-April 1996.